

Competitive charge-remote and anion-induced fragmentations of the non-8-enoate anion. A charge-remote reaction which co-occurs with hydrogen scrambling

PERKIN
2

Suresh Dua,^a John H. Bowie,^{*,a} Blas A. Cerda,^b Chrys Wesdemiotis,^b Mark J. Raftery,^a Julian F. Kelly,^a Mark S. Taylor,^a Stephen J. Blanksby^a and Mark A. Buntine^a

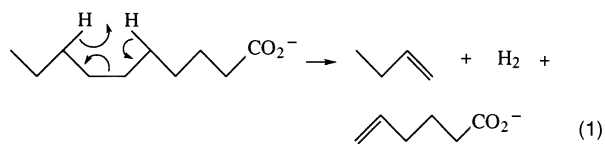
^a Department of Chemistry, The University of Adelaide, South Australia, 5005, Australia

^b Department of Chemistry, The University of Akron, Akron, Ohio 44325-3601, USA

The non-8-enoate anion undergoes losses of the elements of C₃H₆, C₄H₈ and C₆H₁₂ on collisional activation. The mechanisms of these processes have been elucidated by a combination of product ion and labelling (²H and ¹³C) studies, together with a neutralisation reionisation mass spectrometric study. These studies allow the following conclusions to be made. (i) The loss of C₃H₆ involves cyclisation of the enolate anion of non-8-enoic acid to yield the *cyclopentyl* carboxylate anion and propene. (ii) The loss of 'C₄H₈' is a charge-remote process (one which proceeds remote from the charged centre) which yields the pent-4-enoate anion, butadiene and dihydrogen. This process co-occurs and competes with complex H scrambling. (iii) The major loss of 'C₆H₁₂' occurs primarily by a charge-remote process yielding the acrylate anion, hexa-1,5-diene and dihydrogen, but in this case no H scrambling accompanies the process. (iv) It is argued that the major reason why the two charge-remote processes occur in preference to anion-induced losses of but-1-ene and hex-1-ene from the respective 4- and 2-anions is that although these anions are formed, they have alternative and lower energy fragmentation pathways than those involving the losses of but-1-ene and hex-1-ene; *viz.* the transient 4-anion undergoes facile proton transfer to yield a more stable anion, whereas the 2-(enolate) anion undergoes preferential cyclisation followed by elimination of propene [see (i) above].

Introduction

Collision-induced loss of a neutral from an even-electron negative ion in the gas phase often involves reaction involving the charged centre.^{1,2} There are also fragmentations of even-electron anions which are 'charge-remote', *viz.* reactions which occur remote from the charged centre. Amongst the latter are some radical losses which form stabilised radical anions.^{3,4} Substantiated reports of charge-remote reactions involving the loss of even-electron neutrals from even-electron anions are not common. The classical charge-remote mechanistic proposal for alkanolate anions is shown in reaction (1). This was first



proposed by Adams and Gross,⁵⁻⁸ but the mechanism has been questioned.⁹⁻¹¹ Support for the charge-remote mechanism has been provided by Cordero and Wesdemiotis¹² who have used neutralisation reionisation mass spectrometry (NRMS) to identify butene as a neutral product of the reaction shown in reaction (1). This charge-remote process has a large activation barrier; estimates range from *ca.* 200 kJ mol⁻¹ (experimental⁵⁻⁸) to 385 kJ mol⁻¹ (computational¹³).

This paper reports the fragmentations of the non-8-enoate anion, *i.e.* a system similar to the alkanolate shown in reaction (1), except that it has double bond functionality at the opposite end of the molecule to the carboxylate moiety. We anticipated that collision-induced transfer of a proton from the allylic position to the carboxylate anion would yield an allylic anion, and

that this should result in competition between charge-remote fragmentation of the carboxylate anion, and anion-directed fragmentation from the allylic centre. We will show that both charge-remote and anion induced processes do indeed occur in this system, but not as a consequence of fragmentation of an allylic anion.

Results and discussion

We have described above why we chose to study an enoate anion for this study. The first task is to choose which enoate anion is the most suitable for study. The mass spectra of a number of such anions are listed in Table 1. The spectra of the lower homologues are dominated by loss of carbon dioxide and are not suitable for this study. In contrast, the higher homologues show the type of losses previously noted in the spectra of alkanolate anions,^{5-7,12} for example, losses of the elements of C₃H₆, C₄H₈ and C₆H₁₂. In principle, these losses could all be charge-remote reactions analogous to that shown in reaction (1), except of course that the neutral products will be a diene and dihydrogen. We have chosen to probe the mechanisms of these processes using the non-8-enoate anion as a suitable example. The investigation uses a combination of product ion, labelling (D and ¹³C), neutral reionisation mass spectrometry (NRMS) and computational studies.

(a) The evidence based on product ion and labelling studies

The collision-induced negative chemical ionisation tandem mass spectrum (MS/MS) of the (M - D)⁻ ion of CH₂=CH-(CH₂)₆CO₂D is recorded in Fig. 1. The first part of this investigation involves the identification of the structures of the product ions formed following losses of 'C₃H₆', 'C₄H₈' and 'C₆H₁₂'. This was done by comparing (i) MS/MS/MS fragmentation

Table 1 MS/MS data from $\text{CH}_2=\text{CH}(\text{CH}_2)_n\text{CO}_2^-$ ions

$\text{CH}_2=\text{CH}(\text{CH}_2)_n\text{CO}_2^-$ <i>n</i>	Loss									Formation ' CH_2CO_2^- '
	H·	H ₂	H ₂ O ^a	CO ₂	C ₃ H ₆	C ₄ H ₈	C ₅ H ₁₀	C ₆ H ₁₂	C ₈ H ₁₆	
1	100		3	88						5
2	65	5	10	100						7
3	100	10	34	29	2					10
4	100	15	72			8				1
5	100	20	16		17		5			2
6	54	5	72		100	48	3	56		9
8	22		51		100	39	14	10	10	5

^a The loss of H₂O is a standard reaction of carboxylate species and proceeds following proton transfer to form the enolate anion.¹⁴ To take a specific example relevant to the enoic acids: $\text{CH}_2=\text{CHCH}_2\text{CD}_2\text{CO}_2^-$ loses HOD and D₂O in the ratio 2:1. The processes are as follows: $\text{CH}_2=\text{CHCH}_2\text{CD}_2\text{CO}_2^- \rightarrow \text{CH}_2=\text{CHCH}_2\text{C}^-\text{DCO}_2\text{D} \rightarrow [(\text{CH}_2=\text{CHCH}_2\text{CD}=\text{C}=\text{O}) \text{DO}^-] \rightarrow \text{CH}_2=\text{CH}^-\text{CHCD}=\text{C}=\text{O} + \text{HOD}$ and $\text{CH}_2=\text{CHCH}_2\text{C}^-\text{CO}^- + \text{D}_2\text{O}$.

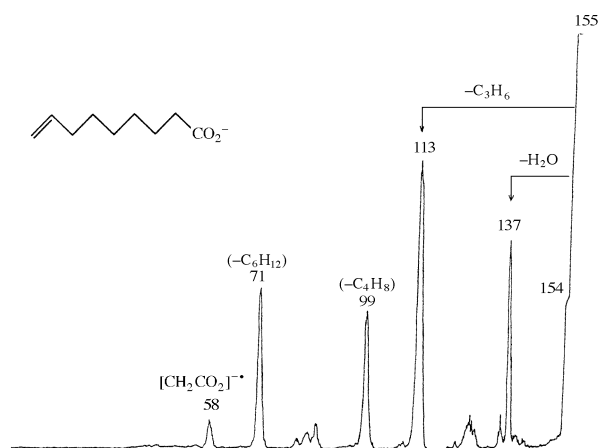
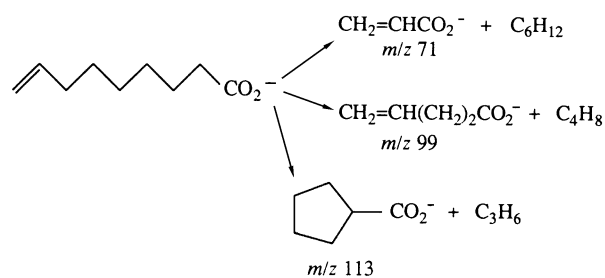


Fig. 1 The collision-induced negative chemical ionisation tandem mass spectrum (MS/MS) of the (M - D)⁻ ion of $\text{CH}_2=\text{CH}(\text{CH}_2)_6\text{CO}_2\text{D}$. VG ZAB 2HF instrument. For experimental conditions, see Experimental section.

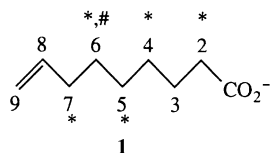
data of each product anion [using an MS 50 TA instrument (through the courtesy of Dr R. N. Hayes and Professor M. L. Gross)] and (ii) MS/MS fragmentation data of source formed product ions (using the VG ZAB 2HF instrument), with the MS/MS data of known ions produced by deprotonation of the appropriate neutral molecules. These data are recorded in Table 2. Results are summarised in Scheme 1. (*B²/E*) Linked scans of



Scheme 1

source formed *m/z* 71, 99 and 113 confirm that each is formed directly from the parent (M - H)⁻ ion.

The product ions shown in Scheme 1 which result from the losses of 'C₄H₈' and 'C₆H₁₂' are those that would be formed from the appropriate charge-remote process [*cf.* reaction (1)].

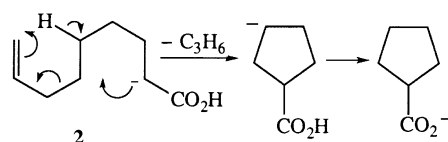


1

However, if the loss of 'C₃H₆' involves a 'charge-remote' process, the ionic product will be $\text{CH}_2=\text{CH}(\text{CH}_2)_3\text{CO}_2^-$. The data in Table 2 identify the product ion as the cyclopentyl carboxylate anion and therefore the loss of C₃H₆ must involve a cyclisation process.

We now wish to study the losses of 'C₃H₆', 'C₄H₈' and 'C₆H₁₂' in detail, and to assist with this endeavour, we have prepared carboxylate anions from five D₂ compounds [those indicated by an * in 1] and one ¹³C compound [that depicted by # in 1]. The MS/MS data derived from all labelled species are recorded in Table 3.

The cyclisation process—loss of C₃H₆. It has already been shown that the product anion of this process is the cyclopentyl carboxylate anion. The deuterium labelling results indicate that both the hydrogens at the 7 position and one hydrogen at position 5 are lost as part of C₃H₆. These data may be rationalised as shown in Scheme 2. Transfer of a proton from position 2 to

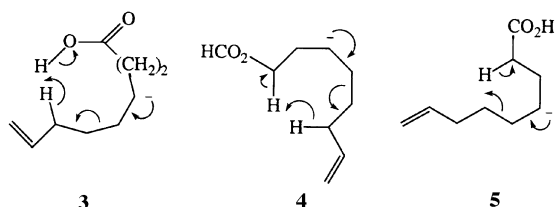


Scheme 2

the carboxylate anion produces the key enolate intermediate (2), which undergoes the cyclisation process shown. We have drawn the cyclisation process [see intermediate 2] in synchronous fashion because of the deuterium labelling results {the alternative stepwise process in which an intermediate [(*cyclo*C₅H₉CO₂H)⁻CH₂CH=CH₂] decomposes to yield *cyclo*-C₅H₉CO₂⁻ and CH₃CH=CH₂, would involve the loss of one H from position 2 (the precursor enolate anion is formed following proton transfer from position 2 to the carboxylate anion centre), not, as observed, from position 5}.

The losses of 'C₄H₈' and 'C₆H₁₂'. The two most plausible mechanisms for the loss of 'C₄H₈' are the charge-remote reaction (2)†

† There are anionic processes like those summarised in formulae (3) and (4), which would give the same products as those formed by charge-remote process (2). These processes are less favourable on energetic grounds than that shown in reaction (3). In addition, we will show later, that such ionic processes do not occur because the precursor 4-anion preferentially undergoes facile proton transfer to form carboxylate (and enolate) anions.

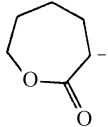
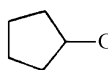


3

4

5

Table 2 MS/MS and MS/MS/MS data for some product ions from the non-8-enoate anion

Precursor ion (<i>m/z</i>)	Product ion (<i>m/z</i>)	Spectrum type	Spectrum [<i>m/z</i> (loss) abundance]
CH ₂ =CH(CH ₂) ₆ CO ₂ ⁻ (155)	-C ₃ H ₆ (113)	MS/MS/MS ^a	111 (H ₂) 100, 71 (C ₃ H ₆) 60
CH ₂ =CH(CH ₂) ₃ CO ₂ ⁻ (113)		MS/MS	111 (H ₂) 100, 71 (C ₃ H ₆) 65, 44 (C ₅ H ₉) 4
CH ₃ CH ₂ CH=CHCH ₂ CO ₂ ⁻ (113)		MS/MS	112 (H ⁺) 100, 111 (H ₂) 10, 95 (H ₂ O) 34, 71 (C ₃ H ₆) 2
CH ₃ (CH ₂) ₂ CH=CHCO ₂ ⁻ (113)		MS/MS	69 (CO ₂) 29, 58 (C ₄ H ₇) 10
 (113)		MS/MS	112 (H ⁺) 18, 97 (CH ₄) 8, 84 (C ₂ H ₅) 4, 69 (CO ₂) 100, 67 (CO ₂ + H ₂) 4, 58 (C ₄ H ₇) 2, 53 (CO ₂ + CH ₄) 3, 44 (C ₅ H ₉) 3
 (113)		MS/MS	112 (H ⁺) 8, 111 (H ₂) 2, 95 (H ₂ O) 100, 85 (28) 8, 83 (CH ₂ O) 64, 71 (C ₃ H ₆) 6, 69 (CO ₂) 2, 57 (C ₄ H ₈) 2, 43 (70) 1
CH ₂ =CH(CH ₂) ₆ CO ₂ ⁻ (155)	-C ₄ H ₈ (99)	MS/MS/MS ^a	111 (H ₂) 100, 71 (C ₃ H ₆) 72, 44 (C ₅ H ₉) 5
CH ₂ =CH(CH ₂) ₂ CO ₂ ⁻ (99)		MS/MS	98 (H ⁺) 70, 81 (H ₂ O) < 10 ^b , 58 (C ₃ H ₅) < 10 ^b , 55 (CO ₂) 100
CH ₂ =CH(CH ₂) ₆ CO ₂ ⁻ (155)	-C ₆ H ₁₂ (71)	MS/MS/MS ^a	98 (H ⁺) 65, 97 (H ₂) 5, 81 (H ₂ O) 10, 58 (C ₃ H ₅) 7, 55 (CO ₂) 100
CH ₂ =CHCO ₂ ⁻ (71)		MS/MS	70 (H ⁺) 100, 27 (CO ₂) 35
		MS/MS	70 (H ⁺) 100, 44 (C ₂ H ₃) 4, 27 (CO ₂) 29

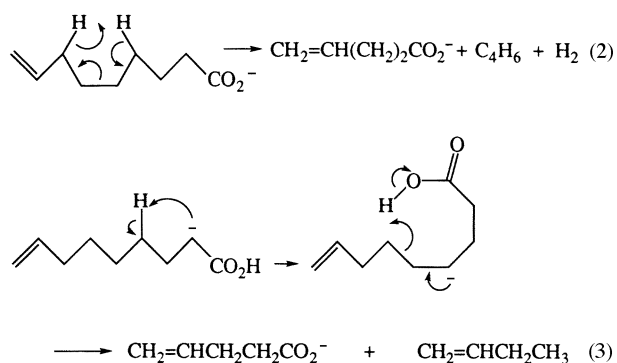
^a The MS/MS/MS spectra are weak: peaks < 5% are lost in baseline noise. ^b The spectra are weak—the abundances of these peaks are only approximate.

Table 3 MS/MS data for labelled non-8-enoate anions

Precursor ion (<i>m/z</i>)	Spectrum [<i>m/z</i> (loss) abundance]
CH ₂ =CH(CH ₂) ₅ CD ₂ CO ₂ ⁻ (157)	156 (H ⁺) 55, 155 (D ⁺) 32, 138/137 ^a (HOD, D ₂ O) 15, 115 (C ₃ H ₆) 100, 101 (C ₄ H ₈) 30 ^b , 102 (C ₄ H ₇ D) 25 ^b , 72 (C ₆ H ₁₁ D) 48, 60 (C ₇ H ₁₃) 22
CH ₂ =CH(CH ₂) ₃ CD ₂ (CH ₂) ₂ CO ₂ ⁻ (157)	156 (H ⁺) 65, 155 (D ⁺) 15, 139 (H ₂ O) 38, 115 (C ₃ H ₆) 100, 101 (C ₄ H ₈) 15, 100 (C ₄ H ₇ D) 30, 71 (C ₆ H ₁₀ D ₂) 45, 58 (C ₇ H ₁₁ D ₂) 24
CH ₂ =CH(CH ₂) ₂ CD ₂ (CH ₂) ₃ CO ₂ ⁻ (157)	156 (H ⁺) 70, 139 (H ₂ O) 28, 114 (C ₃ H ₅ D) 100, 101 (C ₄ H ₈) 15, 100 (C ₄ H ₇ D) 8, 71 (C ₆ H ₁₀ D ₂) 38, 58 (C ₇ H ₁₁ D ₂) 18
CH ₂ =CHCH ₂ CD ₂ (CH ₂) ₄ CO ₂ ⁻ (157)	156 (H ⁺) 45, 139 (H ₂ O) 22, 115 (C ₃ H ₆) 100, 101 (C ₄ H ₈) 8 ^b , 100 (C ₄ H ₇ D) 15 ^b , 99 (C ₄ H ₆ D ₂) 25 ^b , 71 (C ₆ H ₁₀ D ₂) 52, 58 (C ₇ H ₁₁ D ₂) 25
CH ₂ =CHCD ₂ (CH ₂) ₅ CO ₂ ⁻ (157)	156 (H ⁺) 30, 155 (D ⁺) 30, 139 (H ₂ O) 28, 113 (C ₃ H ₄ D ₂) 100, 100 (C ₄ H ₇ D) 15 ^b , 99 (C ₄ H ₆ D ₂) 29 ^b , 71 (C ₆ H ₁₀ D ₂) 38, 58 (C ₇ H ₁₁ D ₂) 18
CH ₂ =CHCH ₂ ¹³ CH ₂ (CH ₂) ₄ CO ₂ ⁻ (156)	155 (H ⁺) 50, 138 (H ₂ O) 15, 114 (¹² C ₃ H ₆) 100, 99 (¹² C ₃ ¹³ CH ₈) 28, 71 (¹² C ₅ ¹³ CH ₁₂) 12, 58 (¹² C ₆ ¹³ CH ₁₃) 5

^a Composite peak not resolved. ^b Peaks not fully resolved.

and the anionic process (3).[‡] Deuterium labelling studies should resolve the problem as to which of processes (2) and (3) is operative. In practice, this turns out not to be the case, since the deuterium labelling data [Table 3, and *cf.* 1] indicate a particularly complex scenario. These data show that hydrogens at positions 2, 4, 5, 6 and 7 have partially scrambled prior to or during the loss of 'C₄H₈'. Hydrogen scrambling in anion systems can, in principle, occur by one of two general processes, *viz.* (i) by specific proton transfer processes occurring to particular anionic sites in the molecule, or (ii) by some type of skeletal rearrangement of the carbon skeleton, or (iii), some combination of both (i) and (ii). The latter scenario is reminiscent of the fragmentations of positively charged long chain carboxylate



[‡] An alternative anionic process involves the reaction of the 4-anion shown in (5).[†] This would result in the formation of but-1-ene and the enolate anion of pent-4-enoic acid. We were unable to find a transition state for this reaction using AM1 calculations and have not considered the process further.

esters, where both H and C rearrangements abound.¹⁵ We prepared the 6-¹³C labelled derivative of non-8-enoic acid in order to distinguish between these possibilities. If carbon skeletal rearrangement is occurring in this negative ion system, both ¹²C₃¹³CH₈' and ¹²C₄H₈' will be lost from the 6-¹³C labelled

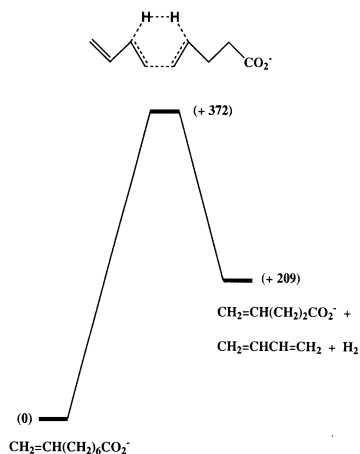


Fig. 2 Semi-empirical AM1 calculations for charge-remote reaction (2). Energy (kJ mol^{-1}) reaction coordinate plot. For computational procedures, see Experimental section.

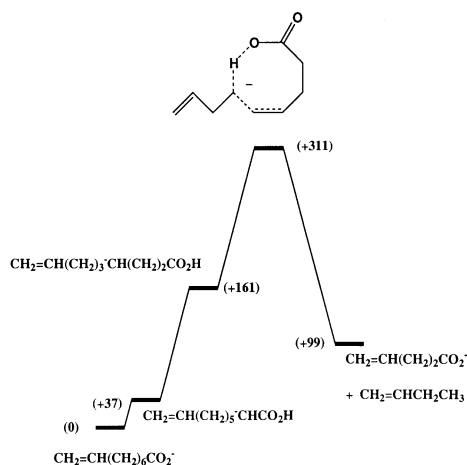


Fig. 3 Semi-empirical AM1 calculations for anionic mechanism reaction (3). Energy (kJ mol^{-1}) reaction coordinate plot.

parent anion. The $(M - H)^-$ ion from $6\text{-}^{13}\text{C}$ -non-8-enoic acid shows exclusive loss of $^{12}\text{C}_3\text{ }^{13}\text{CH}_8^-$; no carbon scrambling precedes or accompanies this or any other fragmentation (see Table 3).

Since we cannot distinguish between reactions (2) and (3) by deuterium labelling, perhaps computational studies may assist. We are not in a position to do high level *ab initio* calculations with systems of such complexity, but estimates of the reaction coordinate profiles for reactions (2) and (3) have been made using semi-empirical calculations (at AM1 level) using GAUSSIAN 94¹⁶ and GAMESS-US¹⁷ (see Experimental section for full details of the procedures used), and these are summarised in Figs. 2 and 3. The data shown in Figs. 2 and 3 should only be used qualitatively, but they do indicate (i), that both processes are energetically unfavourable with high activation barriers [an earlier AM1 calculation of the activation energy of a charge-remote reaction of an alkanolate anion gave a value of 385 kJ mol^{-1} (*cf.* the value in Fig. 2 of 372 kJ mol^{-1}), even though the value was nominally reduced using an experimental correction¹³], and (ii) the anionic process has the lower barrier to the transition state, it is less endothermic overall, but it is the more complex in terms of the number of steps involved. It would be unwise using these data, to propose which of reactions (2) or (3) is the more kinetically favoured.

Turning now to the loss of $^{\cdot}\text{C}_6\text{H}_{12}$: this process could occur by either the charge-remote reaction (4) or from the enolate anion as shown in reaction (5). Since the same hydrogens are eliminated in both processes, deuterium labelling will not distinguish between the two possibilities. The data in Table 3 con-

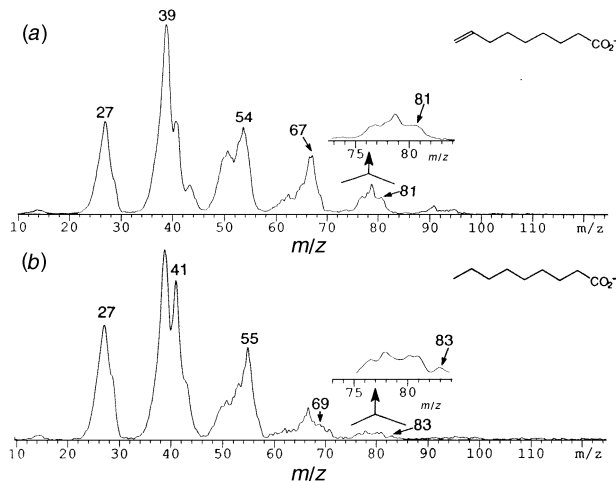
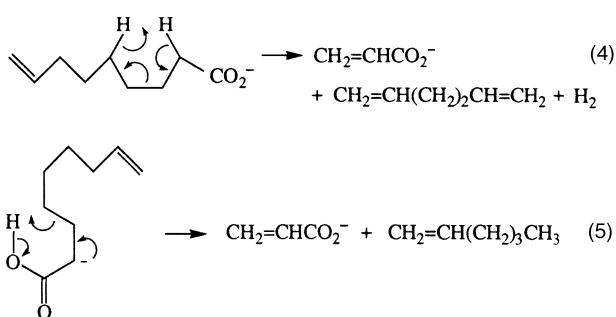


Fig. 4 $^-\text{N}_x\text{R}^+$ spectra of the CID neutrals from (a) the non-8-enoate anion, and (b) the nonanoate anion. VG AutoSpec instrument. For experimental procedures, see Experimental section.



firm the hydrogens involved in the loss of $^{\cdot}\text{C}_6\text{H}_{12}$. No detectable hydrogen scrambling competes with this loss.

The evidence to date does not allow us to differentiate between charge-remote and anion-induced mechanisms for $^{\cdot}\text{C}_4\text{H}_8$ or $^{\cdot}\text{C}_6\text{H}_{12}$ loss.

(b) The evidence based on neutralisation reionisation mass spectrometry

The charge-remote and anionic processes described above can be differentiated based on the neutral molecules they release. For example, the charge-remote reaction (2) produces butadiene plus dihydrogen, whereas the anionic mechanism reaction (3) yields but-1-ene. Which neutrals are cleaved can be found by a NRMS-type experiment, *i.e.* by post-ionising the neutral CID losses and directly detecting them in the corresponding neutral fragment-reionisation, $^-\text{N}_x\text{R}^+$, spectrum.^{12,18} That of the non-8-enoate anion is shown in Fig. 4(a).

For the interpretation of this spectrum, it is important to realise that all neutrals eliminated from the collisionally-activated non-8-enoate precursor anion (see Fig. 1) are post-ionised simultaneously. Each of the neutrals produces several ions upon collision-induced dissociative ionisation (CIDI),¹⁹ the resulting $^-\text{N}_x\text{R}^+$ spectrum arising by superimposition of the individual CIDI spectra.¹⁸ Because of this convolution, spectral interpretation and structural assignments are substantially facilitated if the $^-\text{N}_x\text{R}^+$ spectrum of the unknown [Fig. 4(a)] is compared against the collisional ionisation spectra of relevant reference molecules. An alkene and an alkadiene [Figs. 5(a) and 5(b)] as well as the neutral losses from the saturated nonanoate anion [see Fig. 4(b)] were chosen as the pertinent references in this case and will be discussed first.

Collisional ionisation spectra of hex-1-ene and hexa-1,5-diene. Depending on the decomposition mechanisms of the non-8-enoate anion (see above), the major neutral CID fragments are either alkenes or alkadienes. The types of ions formed upon collisional ionisation of these neutrals can be found by

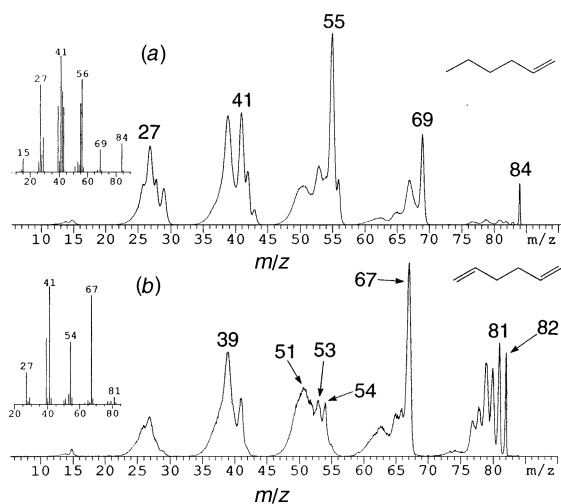


Fig. 5 $^+NR^+$ spectra of the molecular cations from (a) hex-1-ene and (b) hexa-1,5-diene. VG AutoSpec instrument.

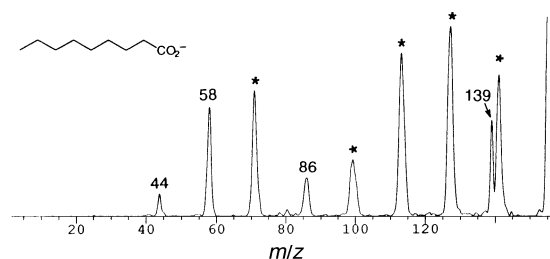


Fig. 6 The CID mass spectrum of the nonanoate anion. VG AutoSpec instrument.

neutralisation-reionisation ($^+NR^+$) of their molecular ions. $^+NR^+$ experiments were conducted with hexa-1,5-diene and hex-1-ene, the larger neutral fragments generated by reactions (4) and (5). Owing to the high kinetic energy, and hence superior transmission and reionisation efficiencies of large neutrals, such moieties generally provide dominant contributions to N_fR^+ spectra.¹⁸

The $^+NR^+$ spectrum of ionised hex-1-ene [Fig. 5(a)] contains a prominent alkenyl ion series, *viz.* $C_nH_{2n-1}^+$ (m/z 27, 41, 55, 69). These ions, which also appear in the EI spectrum of hex-1-ene [inset in Fig. 5(a)],²⁰ are diagnostic for alkenes.²¹ The given alkenyl ions are less important or even absent in the $^+NR^+$ spectrum of ionised hexa-1,5-diene [Fig. 5(b)]. Instead, this spectrum includes a sizeable $C_nH_{2n-3}^+$ series (m/z 39, 53, 67, 81) and other highly unsaturated ions, consistent with the higher degree of unsaturation in the diene.²¹ Highly unsaturated fragments also dominate the EI spectrum of hexa-1,5-diene²⁰ [see inset in Fig. 5(b)]. It can be seen from Fig. 5, that alkenes and alkadienes can be distinguished from a consideration of their collisional ionisation products. It should be noted that the relative fragment ion abundances in $^+NR^+$ and EI spectra differ: this is a consequence of the different internal energy distributions deposited in parent ions by neutralisation-reionisation compared with electron ionisation.²² Thus collisional ionisation reference spectra are most suitable for comparisons with N_fR^+ data.

CID neutrals from the nonanoate anion. The majority of the fragment ions generated upon CID of the $(M-H)^-$ ion from the saturated nonanoic acid correspond to nominal C_nH_{2n+2} losses (marked by an * in Fig. 6). The only important fragments which do not belong to this series are those at m/z 139 (H_2O loss), 86 ($C_5H_{11}^{\cdot}$ loss), 58 ($C_7H_{15}^{\cdot}$ loss) and 44 ($C_8H_{17}^{\cdot}$ loss). Overall, the C_nH_{2n+2} losses make up the largest fraction of the neutral CID fragments and should therefore be the principle contributor of the ions observed in the $^+NR^+$ spectrum [Fig. 4(b)]. The latter contains a relatively abundant alkenyl series

$C_nH_{2n-1}^+$ (m/z 27, 41, 55, 69 and 83), but much less (if any) alkyl ions $C_nH_{2n+1}^+$ (m/z 29, 43, 57, 71 and 85). These spectral characteristics reveal that the formal C_nH_{2n+2} losses cannot be alkanes or alkyl radicals plus H^{\cdot} , because such species would have produced considerable $C_nH_{2n+1}^+$ after reionisation.¹² As discussed in the foregoing section for hex-1-ene, alkenyl ions are diagnostic of alkenes.^{12,21} Thus the $^+NR^+$ data indicate that the major neutrals eliminated from the nonanoate anion are $C_nH_{2n} + H_2$, in agreement with the charge-remote fragmentation depicted in reaction (1). Parallel conclusions were reached from the $^+NR^+$ data of other saturated fatty acids.¹²

The relative intensities in the reference $^+NR^+$ spectrum of hex-1-ene and the $^+NR^+$ spectrum of nonanoate [Figs. 5(a) and 4(b)] do not match. This is because the latter also contains contributions from other smaller alkenes as well as from other CID neutrals (see below). Also, alkenes formed by charge-remote fragmentations are energised because of the large reverse activation energy associated with such processes (*cf.* Fig. 2). This explains why $C_2H_{<2n-1}^+$ fragments, which lie higher in energy than $C_2H_{2n-1}^{+23}$ are more dominant in the $^+NR^+$ spectrum [Fig. 4(b)] than in the reference $^+NR^+$ spectrum [Fig. 5(a)]. For the same reason, alkene molecular ions ($C_nH_{2n}^{\cdot+}$) have a lower relative abundance in the $^+NR^+$ spectrum than in reference $^+NR^+$ spectra. For example, compare m/z 84 ($C_6H_{12}^{\cdot+}$) in Figs. 4(b) and 5(a) (the peak height of $C_6H_{12}^{\cdot+}$ is artificially enhanced in the reference $^+NR^+$ spectrum owing to the small peak width of precursor ions, which are not subject to kinetic energy release). In contrast, the $C_6H_{12}^{\cdot+}$ peak in the $^+NR^+$ spectrum is much wider because it originates from the larger nonanoate ion, and through a process of large reverse activation energy that leads to substantial kinetic energy release).

Three nominal radical losses are observed, namely the losses of $C_5H_{11}^{\cdot}$, $C_7H_{15}^{\cdot}$ and $C_8H_{17}^{\cdot}$ (see Fig. 6). Reionised $C_5H_{11}^{\cdot}$ yields a detectable $C_5H_{11}^+$ ion (m/z 71), whereas only a trace of $C_7H_{15}^+$ (m/z 99) is formed, and there is no $C_8H_{17}^+$ (m/z 113) above noise level. It is possible that the larger radicals decompose more extensively upon post-ionisation. More likely, the CID ions of m/z 58 and 44 are not formed in one step by elimination of $C_7H_{15}^{\cdot}$ or $C_8H_{17}^{\cdot}$ respectively, but originate by consecutive processes, *e.g.* from m/z 86 by losses of C_2H_4 or C_3H_6 .

CID neutrals from the non-8-enoate anion. Comparison of the $^+NR^+$ spectra of the non-8-enoate and nonanoate anions [Figs. 4(a) and 4(b)] shows that the former contains more unsaturated product ions. Fig. 4(a) includes dominant peaks at m/z 54, 67 and 81 but barely any heavier ions within the corresponding peak groups. These products (several of which belong to the $C_nH_{2n-3}^+$ series) also appear in the $^+NR^+$ spectrum of hexa-1,5-diene [Fig. 5(b)] and are characteristic for alkadienes. The small relative abundances of m/z 55, 69 and 83 [see insets in Fig. 4(a)], which are indicative of alkenes [see previous section and Fig. 5(a)], further attests that these alkenes are not an important component in the neutral loss mixture released from the non-8-enoate anion.

The sizeable m/z 54 signal ($C_4H_6^{\cdot+}$) in Fig. 4(a) is due to the elimination of butadiene, consistent with the operation of charge-remote reaction (2). Similarly, the negligible relative intensities of m/z 55 and 56 ($C_4H_7^{\cdot+}$ and $C_4H_8^{\cdot+}$) indicate the loss of but-1-ene (C_4H_8) from the non-8-enoate anion to be an unfavourable process.

The abundant peak corresponding to m/z 81 ($C_6H_9^+$) in Fig. 4(a), shows a small shoulder corresponding to m/z 82 ($C_6H_{10}^{\cdot+}$). The presence of these two products confirms that C_6H_{10} is eliminated from the non-8-enoate anion, supporting the operation of charge-remote process 5. That the neutral is hexa-1,5-diene is confirmed by the reference collisional ionisation spectrum shown in Fig. 5(b). All ions present in the reference spectrum are seen in the $^+NR^+$ spectrum of non-8-enoate [Fig. 4(a)]. The abundance ratio of m/z 54:67 is larger in the $^+NR^+$ than the $^+NR^+$ spectrum, because the former includes a contribution from C_4H_6 loss [reaction (2)]. As explained earlier, the large

reverse activation energy of charge-remote reactions supplies excess energy to the neutral products, promoting extensive fragmentation upon reionisation and reducing peak resolution [*cf.* Figs. 4(a) and 5(b)].

The alkenyl ions $C_6H_{11}^+$ and $C_6H_{12}^{*+}$ (m/z 83 and 84) are of very small abundance in the ${}^{-}N_pR^+$ spectrum of the non-8-enoate anion [Fig. 4(a)]. The nonanoate anion loses hexene, and its ${}^{-}N_pR^+$ spectrum [Fig. 4(b)] shows a small peak corresponding to $C_6H_{11}^+$. Based on the relative ratios of m/z 83:81 in Figs. 4(a) and 4(b), we conclude that the loss of hex-1-ene from the non-8-enoate anion is, at best, a minor process compared with that resulting in loss of hexa-1,5-diene.

Thus ${}^{-}N_pR^+$ data are consistent with (i) charge-remote process (2) operating to the exclusion of anionic process (3), and (ii) the operation of charge-remote process (4) with the possibility of a minor contribution from anionic process (5).

Summary and conclusions

The above study shows that competitive charge-remote and anion-induced processes occur following collisional activation of the non-8-enoate anion.

In summary:

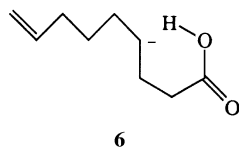
(i) The loss of C_3H_6 is a reaction of the enolate anion (formed following proton transfer to the carboxylate centre), which effects cyclisation to yield the cyclopentyl carboxylate anion and propene. Hydrogen scrambling does not accompany this process.

(ii) The loss of ' C_4H_8 ' is a charge-remote process resulting in the formation of the pent-4-enoate anion together with butadiene and dihydrogen. This reaction co-occurs with extensive proton transfer processes occurring between various carbanions on the carbon skeleton.

(iii) The major process producing overall loss of ' C_6H_{12} ' is a charge-remote reaction which yields the acrylate anion together with hexa-1,5-diene and dihydrogen. A minor accompanying anionic process may involve loss of hex-1-ene. No detectable hydrogen scrambling accompanies this (these) process(es).

In conclusion:

(a) the observation of a charge-remote fragmentation [$-(C_4H_6 + H_2)$] co-occurring with anionic proton scrambling processes is unique in negative ion chemistry. The fact that charge-remote reaction (2) occurs in preference to the anionic process may be rationalised as follows. The 4-carbanion, whose formation is inferred from deuterium labelling data, rearranges by facile proton transfer (to form either or both of the stable enolate or carboxylate anions) in preference to the reaction shown in reaction (3) (there is ample precedent for unstable carbanions undergoing proton transfer to form more stable anions²⁴). We have tested whether such a process is feasible by the use of AM 1 semiempirical calculations. When the 4-carbanion (see Fig. 3) achieves the conformation shown in (6),



proton transfer to form the non-8-enoate anion is immediate: no stable hydrogen bonded intermediate is formed during this process.

(b) The situation concerning loss of ' C_6H_{12} ' is arguably even more complex. NRMS data are consistent with the charge-remote reaction (4) being predominant, and the lack of competitive hydrogen scrambling in this instance implies that the process must have a lower activation barrier than that of the corresponding reaction (2). Further, anionic reaction (5) must have a lower activation barrier than that of the corresponding

reaction (3), since the enolate anion precursor [in reaction (5)] is some 130 kJ mol^{-1} more negative in energy than that shown for the precursor 4-anion [in reaction (3)] (see Fig. 3). This leads to the final question: why then does not anionic reaction (5) occur to the exclusion of charge-remote reaction (4)? The answer must be that the enolate anion preferentially undergoes the cyclisation process already described (see Scheme 2) rather than reaction (5).

Experimental

Mass spectrometric methods

Collisional activation (CID) mass spectra (MS/MS) were determined with a VG ZAB 2HF mass spectrometer.²⁵ Full operating details have been reported.²⁶ Specific details are as follows: the chemical ionisation slit was used in the chemical ionisation source, the ionising energy was 70 eV, the ion source temperature was 100°C , and the accelerating voltage was 7 kV. Non-8-enoic acid was introduced into the source *via* the direct probe with no heating [measured pressure of sample 1×10^{-6} Torr (1 Torr = 133.322 Pa)]. Deprotonation was effected using HO^- (from H_2O) or DO^- (from D_2O) for deuterium-labelled derivatives. The measured pressure of H_2O or D_2O was 1×10^{-5} Torr. The estimated source pressure was 10^{-1} Torr. Argon was used in the second collision cell (measured pressure, outside the cell, 2×10^{-7} Torr), giving a 10% reduction in the main beam, equivalent to single collision conditions.

MS/MS/MS tandem mass spectra were measured (through the courtesy of Professor M. L. Gross and Dr R. N. Hayes) with an MS TA 50 mass spectrometer as described previously.²⁷ The pressure of He collision gas in both collision cells was 1×10^{-6} Torr, producing a reduction in the main beam of 30%.

The NRMS-type experiments were conducted with an E_1BE_2 tandem mass spectrometer (VG AutoSpec at Akron) that has previously been described.²⁸ This instrument houses two collision cells (C-1 and C-2) and an intermediate deflector in the interface region between E_1B and E_2 . The carboxylate anions ($M - H$)⁻ from nonanoic acid and non-8-enoic acid were formed by FAB ionisation, using a 20 keV Cs^+ ion gun and triethanolamine as the matrix. The ($M - H$)⁻ precursor anions were accelerated to 8 keV, selected by E_1B and dissociated with He in C-1. CID coproduces ionic and neutral fragments. After exiting C-1, the ionic fragments and any undissociated ($M - H$)⁻ ions were deflected from the beam path, and the remaining neutral losses were post-ionised in C-2 by collision-induced dissociative ionisation with O_2 .¹⁹ The newly formed cations were mass-analysed by E_2 and recorded in the neutral fragment-reionisation, ${}^{-}N_pR^+$, spectrum.^{12,28} The superscripts besides N and R in the N_pR notation designate the charge of the precursor ion (from which the neutrals are eliminated) and the charges of the ultimate product ions (to which the neutrals are reionised), respectively.¹⁸ Neutralisation-reionisation (${}^+NR^+$) spectra of the molecular cations of hex-1-ene and hexa-1,5-diene were measured similarly by replacing He in C-1 (which causes CID) with trimethylamine (which causes charge exchange neutralisation).¹⁸ In these experiments, molecular cations were generated by electron impact, and were accelerated to the kinetic energy with which hex-1-ene and hexa-1,5-diene would be eliminated from 8 keV nonanoate and 8 keV non-8-enoate, respectively (4.2 to 4.3 keV).

Syntheses of unlabelled and labelled precursor molecules

Hex-1-ene, hexa-1,5-diene, but-3-enoic acid, nonanoic acid and ϵ -caprolactam were commercial products. The following compounds were made by reported procedures: pent-4-enoic acid,²⁹ hex-5-enoic acid,³⁰ hept-6-enoic acid,²⁹ oct-7-enoic acid,²⁹ non-8-enoic acid³¹ and cyclopentane carboxylic acid.³²

2,2-[${}^2\text{H}_2$]pent-4-enoic acid. This was prepared as for the unlabelled analogue,²⁹ except that hydrolysis of the precursor

ester was carried out with NaOD and the final acidification by D₂SO₄ in D₂O. Overall yield 75%, D₂ = 90%.

2,2-[²H₂]Non-8-enoic acid. Non-8-enoic acid³³ (0.5 g) was heated under reflux in MeOD–MeONa [Na (0.2 g) in MeOD (5 cm³)] for 15 h. After being cooled to 25 °C, the solvent was removed *in vacuo*, the residue dissolved in water (5 cm³), cooled (0 °C), acidified to pH 1 with aqueous hydrogen chloride (10%), and extracted with diethyl ether (5 cm³). Removal of the solvent gave the desired product (95% yield; D₁ = 10, D₂ = 90%).

4,4-[²H₂]Non-8-enoic acid. Diethyl succinate was reduced³⁴ with lithium aluminium deuteride in refluxing tetrahydrofuran to yield 1,1,4,4-[²H₄]butane-1,4-diol (yield 85%), which was tosylated³⁵ with tosyl chloride§ (1 equiv.) in anhydrous pyridine to yield a mixture of mono- and di-tosylated 1,1,4,4-[²H₄]butane-1,4-diol. The mono-tosylated product was obtained in 60% yield following column chromatography [on silica eluting with diethyl ether–hexane (1.5:8.5)]. The mono-tosylate was coupled³⁶ with pent-4-ene magnesium bromide to yield 4,4-[²H₂]non-8-enol (yield 72%) which was oxidised³⁷ with chromium trioxide to give the desired 4,4-[²H₂]non-8-enoic acid (overall yield 55%; D₂ = 99%).

5,5-[²H₂]Non-8-enoic acid. This was synthesised by a similar methodology as that used above for 4,4-[²H₂]non-8-enoic acid. Glutaric anhydride was reduced with lithium aluminium deuteride to obtain 1,1,5,5-[²H₄]pentane-1,5-diol. Overall yield of 5,5-[²H₂]non-8-enoic acid, 45%; D₂ = 99%.

6,6-[²H₂]Non-8-enoic acid. This was prepared by first coupling³⁸ 4,4-[²H₂]-4-bromobut-1-ene³⁹ with 5-magnesium bromide pentanol tetrahydropyranyl ether³⁸ to obtain 6,6-[²H₂]non-8-enol tetrahydropyranyl ether in 67% yield. 6,6-[²H₂]non-8-enol was formed following deprotection of the tetrahydropyranyl ether with acid,⁴⁰ and then oxidised³⁷ to give 6,6-[²H₂]non-8-enoic acid in 50% yield (D₂ = 99%).

7,7-[²H₂]Non-8-enoic acid. This was synthesised using a similar methodology as that used for 4,4-[²H₂]non-8-enoic acid. 1,1,7,7-[²H₄]heptane-1,7-diol was prepared by reduction of dimethyl pimelate with lithium aluminium deuteride.³⁴ Overall yield of 7,7-[²H₂]non-8-enoic acid, 55% (D₂ = 99%).

6-¹³C-Non-8-enoic acid. The reaction⁴¹ between allyl bromide (1.2 g) and Cu¹³CN (1.1 g, ¹³C = 99%)⁴² gave allyl (¹³C cyanide) in 70% yield. The allyl (¹³C cyanide) was hydrolysed⁴³ to the labelled vinyl acetic acid (65% yield), which was reduced³⁴ with lithium aluminium hydride in refluxing tetrahydrofuran to form 1-¹³C-but-3-en-1-ol in 78% yield. The alcohol was tosylated⁴⁴ with tosyl chloride. The tosylate was purified by column chromatography over silica in diethyl ether–hexane (1.5:8.5), coupled³⁶ with 5-magnesium bromide pentanol tetrahydropyranyl ether³⁸ to yield 6-¹³C-non-8-enol tetrahydropyranyl ether, which was then deprotected to give the alcohol³⁹ and then oxidised³⁷ to 6-¹³C-non-8-enoic acid (overall yield from 1-¹³C-but-3-en-1-ol, 40%; ¹³C = 99%).

Computational methods

Semi-empirical molecular orbital calculations using the AM1 model Hamiltonian⁴⁵ were performed with the GAUSSIAN 94¹⁶ and GAMESS-US¹⁷ systems of programs. Calculations were performed on a variety of computational platforms, including DECStation 5000/25 and Silicon Graphics Indigo² xZ workstations, as well as Thinking Machines CM-5 and Silicon Graphics Power Challenge supercomputers.

Optimised molecular geometries were characterised as local minima or transition states by subsequent vibrational frequency calculations. Molecular geometries representing local minima possess all positive vibrational frequencies; transition states are identified as possessing one (only) imaginary frequency as well as one (only) negative eigenvalue of the Hessian matrix. The zero-point energy for each structure was also

obtained from the frequency calculations. Calculated zero-point energies tend to overestimate actual energies by up to ca. 15% and are therefore scaled by 0.89.⁴⁶ The reaction barriers were determined by comparing zero point-corrected energies of the appropriate local minima and transition state. Intrinsic reaction coordinate (IRC) calculations from the transition state were undertaken to confirm that the calculated transition state geometry does indeed connect the relevant local minima on the overall reaction potential energy surface.

The following computational protocol was employed in this study. Optimised geometries for reactants and products were determined using GAUSSIAN 94. The molecular geometry of the transition state linking local minima on the reaction potential energy surface (Fig. 3) were then determined using the Linear Synchronous Transit (LST) approach.⁴⁷ The structure resulting from an LST calculation was subsequently used as input for a saddle point geometry optimisation using GAMESS. The saddle point geometry determined from the GAMESS calculation was then input, along with the reactant and product geometric specifications, into a QST3 transition state optimisation using GAUSSIAN 94. QST3 Transition state optimisations employ the Synchronous Transit-Guided Quasi-Newton (STQN) method developed by Schlegel and co-workers.⁴⁸ Finally, IRC calculations were used to confirm that computed transition state geometries do connect the reactants and products of interest.

Acknowledgements

We thank the Australian Research Council (J. H. B.) and both the National Institutes of Health of the U.S.A., and the Ohio Board of Regents (B. A. C. and C. W.), for the financial support of this project. Two of us (S. D. and M. J. R.) thank the ARC for research associate positions. Our thanks also to Dr R. N. Hayes and Professor M. L. Gross for MS/MS/MS data.

References

- 1 J. H. Bowie, *Mass Spectrom. Rev.*, 1990, **9**, 349.
- 2 J. H. Bowie, in *Experimental Mass Spectrometry*, ed. D. H. Russell, Plenum Press, New York and London, 1994, pp. 1–38.
- 3 P. C. H. Eichinger and J. H. Bowie, *Int. J. Mass Spectrom. Ion Processes*, 1991, **110**, 123.
- 4 S. Dua, J. H. Bowie and J. C. Sheldon, *J. Chem. Soc., Perkin Trans. 2*, 1994, 543.
- 5 J. Adams and M. L. Gross, *J. Am. Chem. Soc.*, 1986, **108**, 6915.
- 6 J. Adams and M. L. Gross, *J. Am. Chem. Soc.*, 1989, **111**, 435, and references cited therein.
- 7 J. Adams, *Mass Spectrom. Rev.*, 1990, **9**, 141.
- 8 M. L. Gross, *Int. J. Mass Spectrom. Ion Processes*, 1992, **118/119**, 137.
- 9 V. H. Wysocki, M. H. Bier and R. G. Cooks, *Org. Mass Spectrom.*, 1988, **23**, 627.
- 10 V. H. Wysocki, M. M. Ross, S. R. Horning and R. G. Cooks, *Rapid Commun. Mass Spectrom.*, 1988, **2**, 214.
- 11 V. H. Wysocki and M. M. Ross, *Int. J. Mass Spectrom. Ion Processes*, 1991, **104**, 179.
- 12 M. M. Cordero and C. Wesdemiotis, *Anal. Chem.*, 1994, **66**, 861.
- 13 M. M. Siegel and N. B. Colthup, *Appl. Spectrosc.*, 1988, **42**, 1214.
- 14 K. M. Downard, J. C. Sheldon, J. H. Bowie, D. E. Lewis and R. N. Hayes, *J. Am. Chem. Soc.*, 1989, **111**, 8112, and references cited therein.
- 15 W. Sonneveld, D. Van der Steen and H. J. J. Pabon, *Recl. Trav. Chim., Pays-Bas*, 1968, **87**, 1110; Ng. Dinh-Nguhen, *Arkiv. Kemi*, 1968, **28**, 289.
- 16 Gaussian 94, Revision C.3, M. J. Frisch, G. W. Trucks, H. B. Schlegel, P. M. W. Gill, B. G. Johnson, M. A. Robb, J. R. Cheesman, T. Keith, G. A. Petersson, J. A. Montgomery, K. Raghavachari, M. A. Al-Latham, V. G. Zakrzewski, J. V. Ortiz, J. B. Foresman, J. Cioslowski, B. B. Stefanov, A. Nanayakkara, M. Challacombe, C. Y. Peng, P. V. Ayala, W. Chen, M. W. Wong, J. L. Andres, E. S. Replogle, R. Gomperts, R. L. Martin, D. J. Fox, J. S. Binkley, D. J. Defrees, J. Baker, J. P. Stewart, M. Head-Gordon, C. Gonzalez and J. A. Pople, Gaussian Inc., Pittsburgh, PA, 1995.

§ Tosyl chloride = 4-methylphenylsulfonyl chloride.

- 17 M. W. Schmidt, K. K. Baldrige, J. A. Boatz, S. T. Elbert, M. S. Gordon, J. H. Jensen, S. Koseki, N. Matsunaga, K. A. Nguyen, S. Su, T. L. Windus, M. Dupuis and J. A. Montgomery, *J. Comput. Chem.*, 1993, **14**, 1347.
- 18 M. J. Polce, S. Beranova, M. J. Nold and C. Wesdemiotis, *J. Mass Spectrom.*, 1996, **31**, 1073.
- 19 P. C. Burgers, J. L. Holmes, A. A. Mommers, J. E. Szulejko and J. K. Terlouw, *Org. Mass Spectrom.*, 1984, **19**, 422.
- 20 F. W. McLafferty and D. B. Stauffer, *Wiley/NBS Registry of Mass Spectral Data*, 1989, Wiley, New York.
- 21 F. W. McLafferty and F. Turecek, *Interpretation of Mass Spectra*, University Science Books, Mill Valley, CA, 4th edn., 1993.
- 22 S. Beranova and C. Wesdemiotis, *J. Am. Soc. Mass Spectrom.*, 1994, **5**, 1093.
- 23 S. G. Lias, J. E. Bartmess, J. F. Liebman, J. L. Holmes, R. D. Levin and W. G. Mallard, *Gas Phase Ion and Neutral Thermochemistry*, *J. Phys. Chem. Ref. Data* 17, 1988, Suppl. 1. The computer-based version was used.
- 24 S. T. Graul and R. R. Squires, *J. Am. Chem. Soc.*, 1990, **112**, 2506 and references cited therein; K. M. Downard, R. N. Hayes and J. H. Bowie, *J. Chem. Soc., Perkin Trans. 2*, 1992, 1815.
- 25 J. K. Terlouw, P. C. Burgers and H. Hommes, *Org. Mass Spectrom.*, 1979, **14**, 307.
- 26 G. W. Adams, J. H. Bowie and R. N. Hayes, *J. Chem. Soc., Perkin Trans. 2*, 1991, 689.
- 27 D. J. Burinsky, R. G. Cooks, E. K. Chess and M. L. Gross, *Anal. Chem.*, 1982, **54**, 295; M. L. Gross, E. K. Chess, P. A. Lyon, F. W. Crow, S. Evans and H. Tudge, *Int. J. Mass Spectrom. Ion Phys.*, 1982, **42**, 574.
- 28 M. J. Polce, M. M. Cordero, C. Wesdemiotis and P. A. Bott, *Int. J. Mass Spectrom. Ion Processes*, 1992, **113**, 35.
- 29 R. P. Linstead and H. N. Rydon, *J. Chem. Soc.*, 1933, 580.
- 30 R. P. Linstead and H. N. Rydon, *J. Chem. Soc.*, 1934, 1995.
- 31 H. Stetter and W. Dierichs, *Chem. Ber.*, 1952, **85**, 1061.
- 32 D. W. Gohen and W. R. Vaughan, *Org. Syn. Coll. Vol. 4*, 1963, 594.
- 33 T. H. Chan and D. Stossel, *J. Org. Chem.*, 1986, **51**, 2423.
- 34 A. Burger, L. Turnbull and J. G. Dinwiddie, *J. Am. Chem. Soc.*, 1950, **72**, 5512.
- 35 A. I. Vogel, *Textbook of Practical Organic Chemistry*, Longman and Green Pty Ltd., 4th edn., 1978, p. 1103.
- 36 G. Fouquet and M. Schlosser, *Angew. Chem., Int. Ed. Engl.*, 1974, **13**, 82.
- 37 E. J. Eisenbraun, *Org. Syn. Coll. Vol. 5*, 1973, 310.
- 38 J. H. Babler and B. J. Invergo, *J. Org. Chem.*, 1979, **44**, 3723.
- 39 A. Padwa, W. F. Rieker and R. J. Rosenthal, *J. Org. Chem.*, 1984, **49**, 1353.
- 40 E. J. Corey, H. Niwa and J. Knolle, *J. Am. Chem. Soc.*, 1978, **100**, 1942.
- 41 J. V. Supniewski and P. L. Salzberg, *Org. Syn. Coll. Vol. 3*, 1955, 851.
- 42 H. J. Barber, *J. Chem. Soc.*, 1943, 79.
- 43 E. Reitz, *Org. Syn. Coll. Vol. 3*, 1955, 851.
- 44 L. Brandsma and H. D. Verknijsse, *Synthesis of Ethylenes, Allenes and Cumulenes*, Elsevier, New York, 1981, p. 223.
- 45 M. J. S. Dewar, E. G. Zebisch and E. F. Healy, *J. Am. Chem. Soc.*, 1985, **107**, 3902.
- 46 W. Hehre, L. Radom, P. v. R. Schleyer and J. A. Pople, *Ab Initio Molecular Orbital Theory*, Wiley, New York, 1986.
- 47 T. A. Halgren and W. N. Lipscomb, *Chem. Phys. Lett.*, 1977, **49**, 225.
- 48 C. Peng and H. B. Schlegel, *Israel J. Chem.*, 1993, **33**, 449.

Paper 6/07437E
 Received 1st November 1996
 Accepted 3rd December 1996